HETEROCYCLES, Vol. 93, No. 2, 2016, pp. 770 - 782. © 2016 The Japan Institute of Heterocyclic Chemistry
Received, 31st August, 2015, Accepted, 30th September, 2015, Published online, 26th October, 2015
DOI: 10.3987/COM-15-S(T)33

RING-CONTRACTIVE AND -CLOSING SKELETAL REARRANGEMENT OF 1,1'-BINAPHTHALENE-2,2'-DIAMINES (BINAMS) INDUCED BY AN IODINE-CONTAINING OXIDANT: SYNTHESIS OF SPIRO[BENZO[*e*]INDOLE-1,1'-INDEN]-2-AMINES AND APPLICATION TO AN AIEE-ACTIVE BF_2 COMPLEX

Masato Okazaki, Kosuke Takahashi, Youhei Takeda,* and Satoshi Minakata*

Department of Applied Chemistry, Graduate School of Engineering, Osaka University, Yamadaoka 2-1, Suita, Osaka 565-0871, Japan. E-mail: takeda@chem.eng.osaka-u.ac.jp, minakata@chem.eng.osaka-u.ac.jp

Abstract – An iodine-containing oxidant-induced ring-contractive and -closing skeletal rearrangement of 1,1'-binaphthalene-2,2'-diamines (BINAMs) to afford spiro[benzo[*e*]indole-1,1'-inden]-2-amines has been discovered. Furthermore, a spiro product was successfully transformed into a novel luminescent spirocyclic BF_2 complex.

Spiro heterocycles are ubiquitous motifs found in natural products,[1] and relatedly, they can serve as leading compounds for the discovery of pharmaceuticals.[2] Also, the successful use of spiro heterocycles as axially chiral ligands in transition-metal-catalyzed reactions represents their importance.[3] Moreover, spiro heterocycles containing π-conjugated fragments are promising candidates for organic optoelectronic materials, because their rigid and sterically demanding perpendicular structures should allow for unique physicochemical properties like high glass transition temperatures (T_g) and high quantum efficiencies in the solid state.[4] Although there have been numerous synthetic methodologies reported for spiro heterocycles,[5] the development of new synthetic reactions that open the door to novel spiro heterocyclic compounds would be desired for further quest for their potential usage.

This paper is dedicated to the celebration of the 75th birthday of Professor Dr. Lutz F. Tietze.

During the course of our studies on the development of novel oxidative transformations of aromatic amines into aza-π-conjugated functional molecules,[6–8] we have recently discovered an iodine-containing oxidant-induced skeletal rearrangement of 1,1'-binaphthalene-2,2'-diamines (BINAMs) (**1**) leading to dibenzo[*a*,*j*]phenazines through the formal C–C bond cleavage and nitrogen migration (Scheme 1, the upper equation).[9] Intriguingly, further pursuit of this reaction system led us to another serendipitous finding that the reactions carried out at a lower temperature (–40 °C) exclusively gave spiro[benzo[*e*]indole-1,1'-inden]-2-amines (**2**) instead of dibenzophenazine products (Scheme 1, the bottom equation). It should be noted that this reaction formally involves the ring-contraction of one naphthalene unit (the disconnection of the C2'–C3' bond and the formation of the C1'–C3' bond) and the ring-closure between C2' and the nitrogen atom on C2 atom. Although similar oxidant-promoted rearrangements of 2,2'-disubstituted 1,1'-binaphthalenes have been reported (1,1'-binaphthalene-2,2'-diols with $FeCl_3 \cdot 6H_2O$[10] and 2'-amino-[1,1'-binaphthalen]-2-ol with $CuCl_2 \cdot 2H_2O$/ethanolamine[11]), there is no report about the variant using BINAMs as a substrate. Herein we present an oxidative skeletal rearrangement approach to a novel class of spiro aza-heterocycles which consist of a benzo[*e*]indole and an indene moieties. Furthermore, a product was successfully derivatized to a new luminogenic compound **7**, which exhibits aggregation-induced emission enhancement (AIEE) property[12] (Scheme 1).

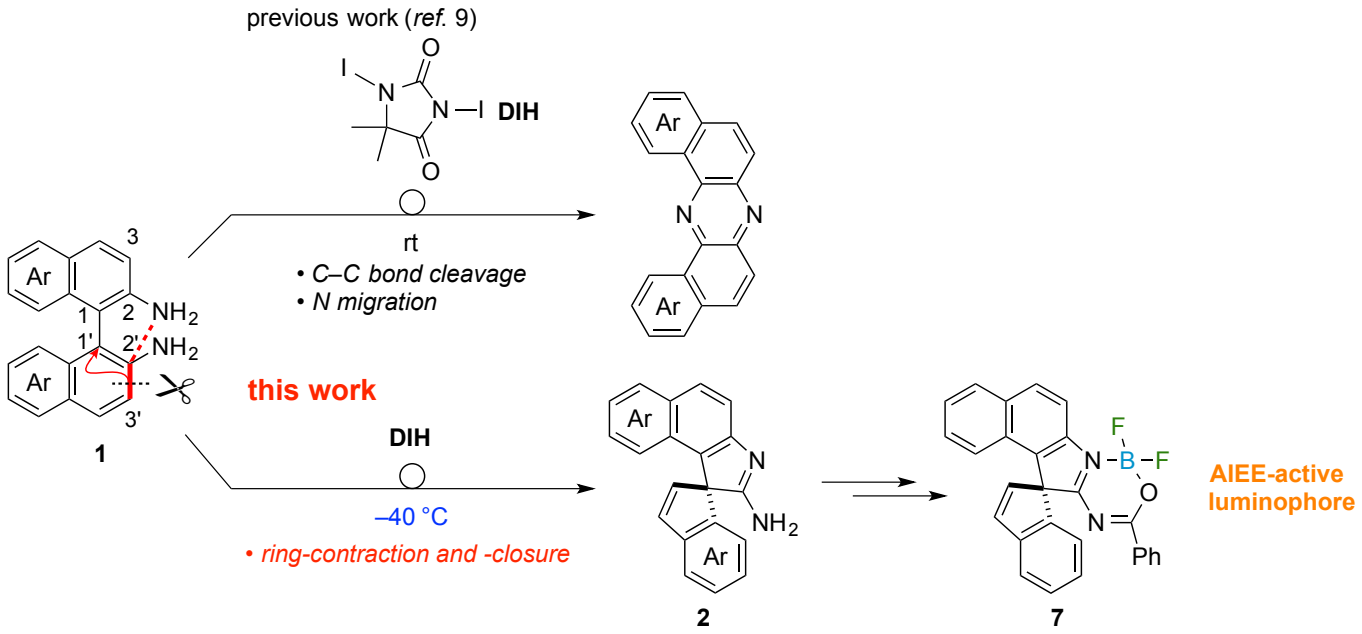

Scheme 1. Temperature-controlled oxidative rearrangements of BINAMs **1**

As briefly mentioned above, the treatment of BINAM (**1a**, 0.2 mmol) with 1,3-diiodo-5,5-dimethylhydantoin (DIH, 0.4 mmol) in MeOH at –40 °C for 3 h gave spiro product **2a** in 50% yield along with the recovery of **1a** in 19% (Equation 1).

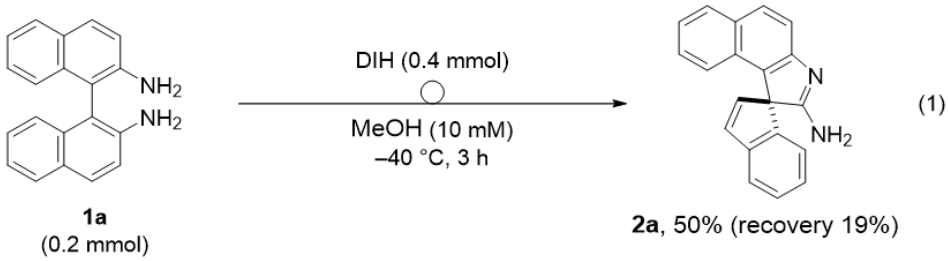

The X-ray crystallographic analysis of the single crystal of **2a**, which was grown from an acetone solution, unambiguously confirmed its geometric structure (Figure 1a).[13] As illustrated, a 1*H*-indenylidene and a 2-amino-1*H*-benzo[*e*]indolylidene groups share the spiro carbon C1, and these aromatic planes are almost perpendicular to each other (dihedral angle: 85.2°). In general, amidine compounds can exhibit prototropic tautomerism, which influences their pK_as and reactivities.[14] The C2–N2 bond (1.308 Å) was shorter than the C2–N1 bond (1.333 Å) by about 0.025 Å, while these bond lengths almost agree with the values of C(sp^2)=N bond (1.298–1.329 Å) and C(sp^2)–NH_2(sp^2) bond (1.336 Å), respectively.[15] The values of these C–N bond lengths are similar to those of spiro[bicyclo[2.2.1]-heptane-2,3'-indol]-2'amine, whose crystallographic structural data are reported in the literature.[16] Furthermore, two hydrogen atoms (H1A and H2B) on the amidino group were located in the difference Fourier map around the N1 atom. These results might indicate that **2a** exists as the tautomer as shown in Equation 1 in the solid state. Another characteristics about **2a** involves a dimeric motif formed by adjacent two molecules through two pairs of intermolecular hydrogen bonding (N1–H1A···N2) in a similar way to a known spiro cyclic amidine.[16]

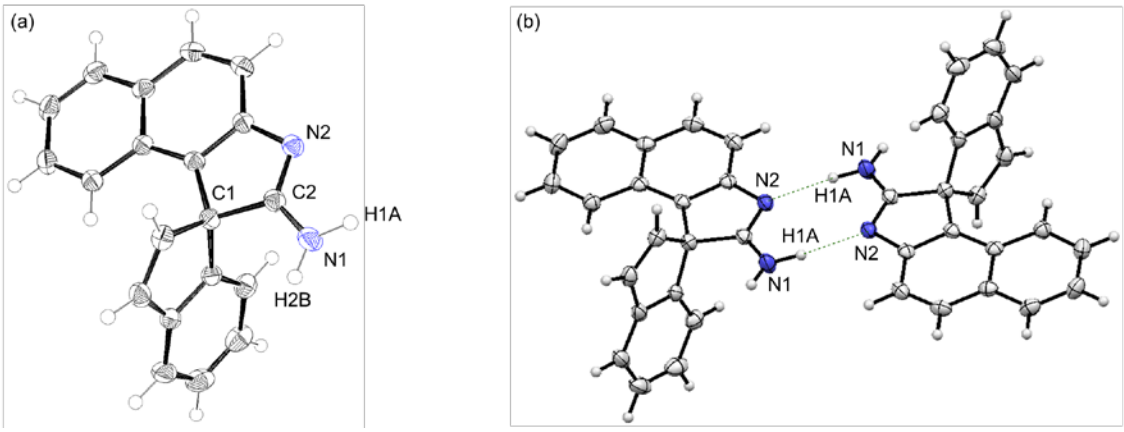

Figure 1. (a) ORTEP diagram of **2a** (Thermal ellipsoids are set at the 50% probability level.); Selected bond length (Å): C2–N1, 1.3333(1); C2–N2, 1.3080(1); (b) A dimeric motif of **2a**

To optimize the reaction conditions, we began by screening reaction parameters using **1a** as a model substrate (Table 1, for the full details, see the Supporting Information). The reaction in acetonitrile gave **2a** in almost the same yield as that in MeOH with a moderate conversion of the starting material **1a** (entry 1). In order to further consume **1a**, reaction time was elongated to 7 h, which enhanced the yield to 69%

(entry 2). However, further extension of reaction time resulted in a lower yield, probably due to the decomposition of **2a** with DIH (entry 3, see the Supporting Information). Oxidants significantly affected the yields of **2a**: *N*-iodosuccinimide (NIS, entry 4) and *N*-iodopyrrolidone (NIPy, entry 5) gave a moderate and a low yields, respectively, whereas *tert*-butyl hypoiodite (*t*-BuOI, entry 6)[6] and 1,3-dibromo-5,5-dimethylhydantoin (DBH, entry 7) did not produce **2a** at all. On one hand, the reported reaction conditions for similar type rearrangements of 1,1'-binaphthalene-2,2'-diols ($FeCl_3 \cdot 6H_2O$)[10] and 2'-amino-[1,1'-binaphthalen]-2-ol ($CuCl_2 \cdot 2H_2O$/ethanolamine)[11] did not give **2a** (see the Supporting Information).

Table 1. The effect of reaction conditions on the oxidative rearrangement of **1a**

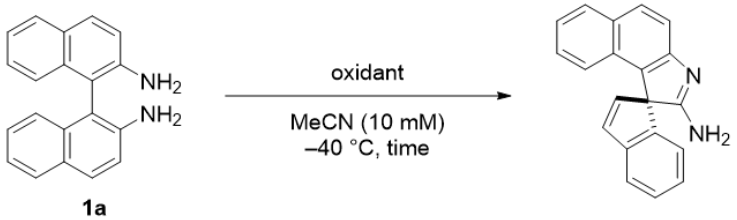

1a (0.2 mmol) → **2a**

entry	oxidant (mmol)	time (h)	yield (%)[a]	recovery (%)[a]
1	DIH (0.4)	3	47[b]	36[b]
2	DIH (0.4)	7	69[b]	17[b]
3	DIH (0.4)	12	43	7
4	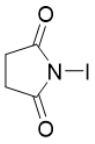 NIS (0.8)	7	45	49
5	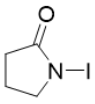 NIPy (0.8)	5	3	55
6	*t*-BuOI (0.8)	7	0	5
7	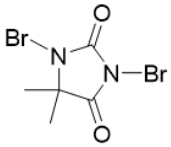 DBH (0.4)	7	0	0

[a] ^{1}H NMR yields. [b] isolated yield.

Having identified the optimized conditions for the oxidative rearrangement, the scope of substrates were surveyed (Table 2). The reaction using 6,6'-di-*n*-butyl-substituted BINAM **1b** (0.1 mmol) in MeOH gave

the expected spiro product **2b** in 40% yield (entry 1), while the employment of MeCN ended in an inferior yield (see the Supporting Information). The treatment of a BINAM bearing 6,6'-dibromo substituents **1c** with DIH provided the corresponding spiro amidine **2c**, albeit in a low yield (13%) (entry 2). Since bromo group can be transformed into various functionalities through transition-metal-catalyzed coupling reactions, **2c** would serve as a building block for the construction of functionalized aza-spiro compounds. Regarding the limitation of substrates, 3,3'-disubstituted BINAMs **1d** (Ph) and **1e** (OMe) were not successful, probably due to steric congestion around the spiro carbon center to be formed. Bianthracene diamine **1f** also failed to provide the desired product **2f** (see the Supporting Information).

Table 2. Substrate scope of the oxidative rearrangement of BINAMs **1**

entry	**1**	R	solvent	time (h)	**2**	yield (%)	recovery (%)
1	**1b**	*n*-Bu	MeOH	3	**2b**	40	20
2	**1c**	Br	MeCN	7	**2c**	13	71

For understanding the mechanistic aspects of the rearrangement, a few experiments were conducted (Scheme 2). The treatment of diamine **3** under the optimized conditions for **1a** did not give the corresponding spiro product **4** (Scheme 2a), suggesting that the existence of naphthalene units in diamine is indispensable for the oxidative rearrangement, and thereby that dearomatization processes could be involved in the reaction pathway. To check the stereochemical outcome of the reaction, optically pure (*R*)-BINAM **1a** (>99% ee) was subjected to the optimized reaction conditions (Scheme 2b). As a result, optically active product (–)-**2a** ($[\alpha]_D^{20}$ –4.00, *c* 1.00, $CHCl_3$)[17] was obtained with a slight loss of enantiopurity (89% ee, HPLC), suggesting that the axial chirality of **1a** was mostly translated into the chirality of **2a** through the reaction. Photo-induced decomposition of 2'-azido-[1,1'-binaphthalen]-2-amine (**5**) effected by the irradiation of UV light (high-pressure mercury lamp) at –40 °C gave spiro compound **2a** in 18% yield (Scheme 2c). Since the photo- and thermal-decomposition of β-naphthyl azides transiently generate β-naphthyl nitrenes, which promptly isomerize to β-naphthazirines with dearomatization, the experimental result would indicate the intermediacy of such β-naphthazirine species through the reaction pathway.[18]

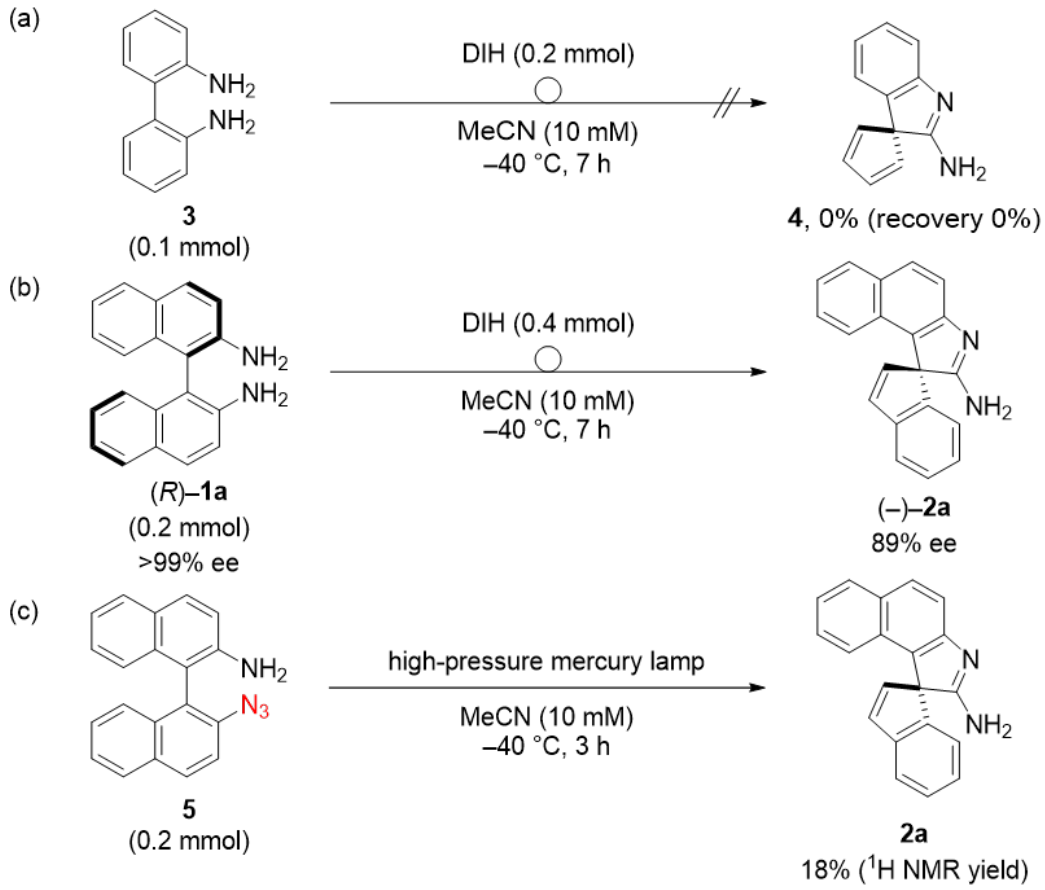

Scheme 2. Mechanistic studies on the oxidative rearrangement of BINAMs

Taking account of the experimental results shown in Scheme 2, possible reaction pathways of the rearrangement of **1a** leading to **2a** are proposed in Figure 2. Hydrogen(s) of an amino group of **1a** would exchange with iodine(s) to give mono- or di-iodinated intermediate **A** in the same way as our previous works,[6,9] which would be dearomatized to give naphthazirine **B** (path a). The resulting azirine would undergo intramolecular nucleophilic attack by the other amino group to give **C**, which should be converted to aziridine **D** through proton transfer.[19] The 3-membered ring of **D** would be opened driven by the release of its strain energy to provide zwitterionic intermediate **E**. A resonance structure of **E** can be drawn like **F**, whose contribution would be more significantly dominated because it would gain more stabilization by the recovery of aromaticity of a naphthalene unit. Aza-pinacol type rearrangement of **F** would generate spiro compound **G**,[20] which then would tautomerize to **2a**. Another pathway leading to **F** that does not involve azirine intermediate could be feasible (path b). With regard to the stereochemical outcome of the reaction, the chiral information of **1a** would be kept through axial-to-central (from **A** to **B**) and central-to-axial (from **F** to **G**) chirality transfer. The reason why a slight degree of enantiopurity was lost through a reaction might be that a racemization process via an intermediate **H** exists.

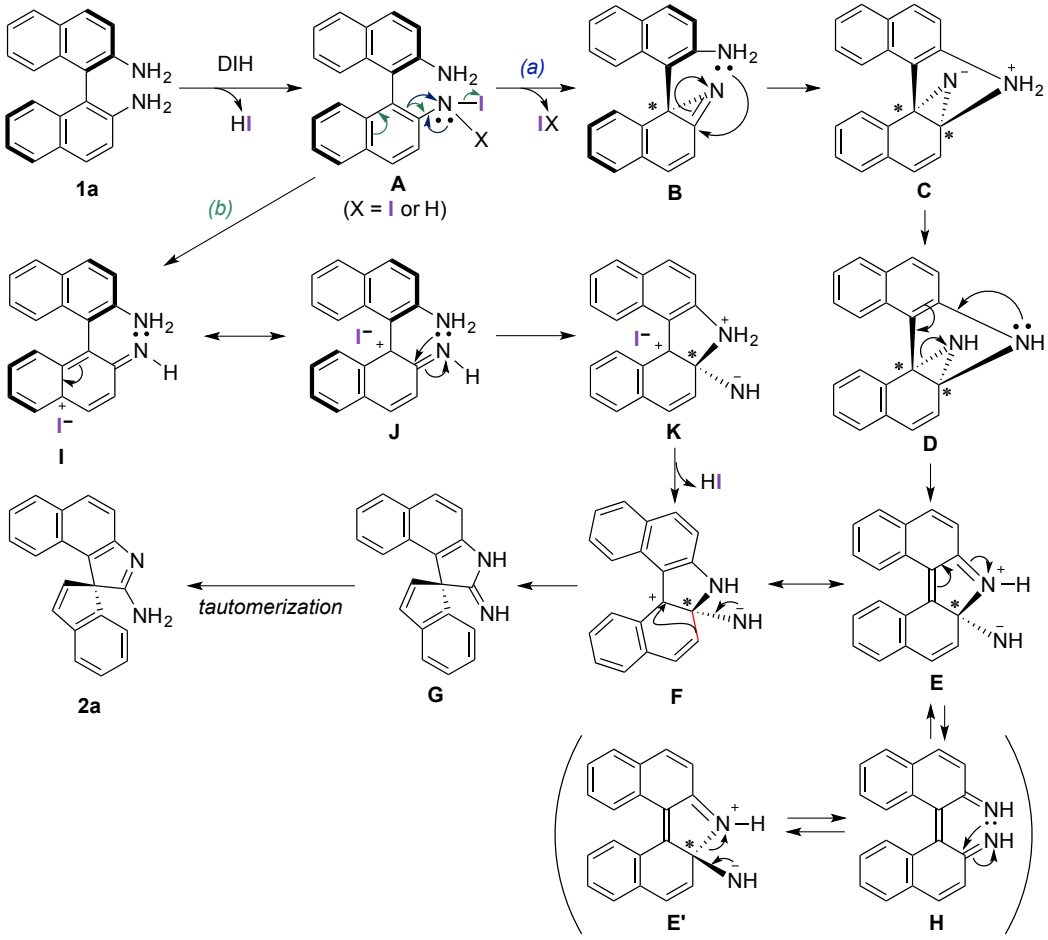

Figure 2. Possible reaction pathways of the oxidative rearrangement of **1a**

Taking advantage of the amidino functionality of rearranged products, **2a** was successfully transformed into BF_2 complex **7** possessing a bidentate N^N^O group (Scheme 3). To date, several examples of BF_2 complexes containing a bidentate N^N^O group have been reported,[21–23] and they have been shown to be promising luminophores in the solid state as well as in the solution.[23] In conjunction with these precedents, we surmised that the BF_2 complex **7** would also serve as an emissive organic solid, because the sterically demanding spiro moiety would avoid intermolecular electronic interactions such as π-π stacking that often cause concentration quenching of emission.[12] Amidine **2a** underwent *N*-acylation with benzoyl chloride to give amide **6** in a moderate yield, which was then converted to BF_2 complex **7** by the treatment with $BF_3{\cdot}Et_2O$ in the presence of Et_3N in dry CH_2Cl_2 at ambient temperature.

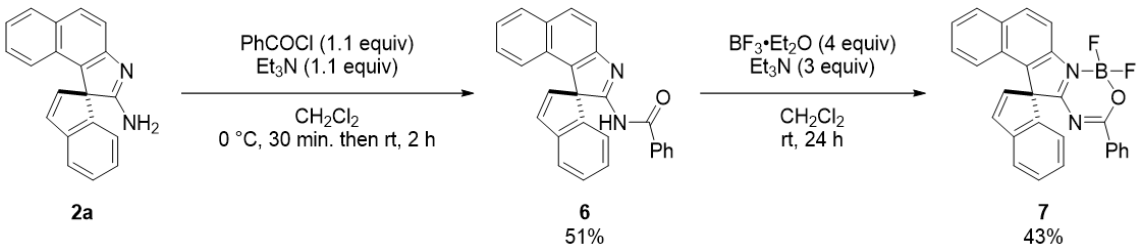

Scheme 3. Synthetic route to N^N^O chelated BF_2 complex **7**

Figure 3a shows the molecular structure of **7** determined by X-ray crystallographic analysis.[24] The BF_2 unit is coordinated by the N2 and O1 atoms, and the B1 center adopts a slightly distorted tetrahedral geometry with the bond angles around the B1 atom (∠X–B1–Y; X, Y = N2, O1, F1, F2) ranging from 105.5(2) to 111.4(3)°. The B1–F1, B1–F2, B1–N2, and B1–O1 distances are 1.368(4), 1.371(4), 1.548(4) and 1.485(4) Å, respectively. The B1–N2 bond is slightly shorter and the B1–O1 slightly longer than those of known N^N^O chelated BF_2 complexes.[22,23] The sum of the interior angles of the boron-containing 6-membered ring is 719.6°, indicating that these atoms are located almost on the same plane. Importantly, this 6-membered heterocycle and the phenyl ring connected to the C21 are nearly coplanar, suggesting the highly extended π-conjugation in the solid state. In fact, effective π-conjugation along the heterocycle–benzene plane was supported by DFT calculations: the LUMO orbital is delocalized over the boron-containing 6-membered ring and the phenyl moiety, and the LUMO energy is significantly decreased (see the Supporting Information). Furthermore, it is noteworthy that any intermolecular π-π close contacts were not observed in the packing structure of **7** (Figure 3b), probably due to the existence of the perpendicular indene moiety. Two 1*H*-indenylidene planes (colored in yellow) are aligned in a slipped face-to-face fashion with the interplanar distance being 2.75 Å, although these planes do not overlap with each other.

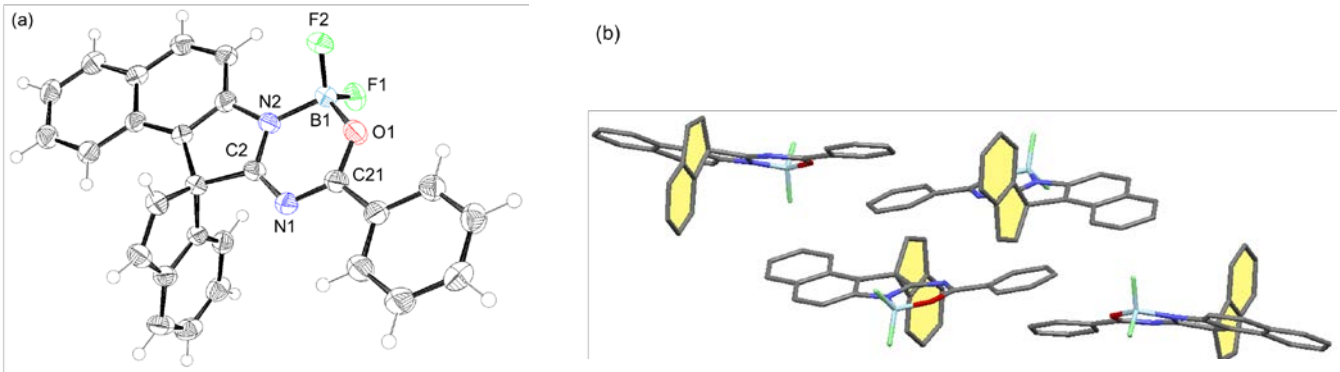

Figure 3. (a) ORTEP diagram of **7** (Thermal ellipsoids are set at the 50% probability level.); Selected bond lengths (Å) and angles (°): B1–F1, 1.368(4); B1–F2, 1.371(4); B1–N2, 1.548(4); B1–O1, 1.485(4); N2–B1–O1, 105.5(2); N2–B1–F1, 110.8(3); N2–B1–F2, 110.0(2); O1–B1–F1, 109.7(3); O1–B1–F2, 109.2(3); F1–B1–F2, 111.4(3); B1–N2–C2, 121.8(3); N2–C2–N1, 125.9(3); C2–N1–C21, 115.5(3); N1–C21–O1, 125.3(3); C21–O1–B1, 125.5(3); (b) Packing structure of **7** (Hydrogen atoms are omitted, and indene planes are painted in yellow for clarity.)

To understand the influence of the complexation with BF_2 moiety, photophysical properties of **2a**, **6**, and **7** were investigated (Figure 4). UV-vis absorption spectrum of a cyclohexane solution of **2a** exhibited weak absorptions (ε ~2900 $M^{-1}cm^{-1}$) in the lower energy region (300–350 nm) and strong absorptions (ε ~23200 $M^{-1}cm^{-1}$) in the higher energy region (250–270 nm) that were ascribed to π-π* transitions by TD-DFT calculations (see the Supporting Information). The *N*-acylation of **2a** drastically increased the molar absorption coefficients in the lower energy region of **6**. Compared with **2a** and **6**, the absorption

edge of **7** exhibited a distinct red-shift (λ_{edge} 470 nm; λ_{edge} of **2a** and **6** were 379 and 408 nm, respectively), and the strong absorptions (ε ~11500 $M^{-1}cm^{-1}$) in the lower energy region (340–450 nm) ascribed to π-π* transition were observed. To investigate the effect of solvent polarity on its photophysical properties, the absorption and emission spectra of dilute solutions of **7** prepared from various solvents were measured (Figure 4b and 4c). Although the absorption spectra became more broadened as the polarity of solvents increased, the maximum absorption wavelengths were almost unchanged in the all solvents tested (Figure 4b). In contrast to the absorption spectra, the maximum emission wavelength (λ_{em}) exhibited slight red-shifts in polar solvents (Figure 4c). A positive but small slope in the plot of the Stokes shifts ($\Delta\nu$, cm^{-1}) against the orientation polarizability (Δf) (the Lippert–Mataga plot)[25] indicates that the variation in the dipole moment of **7** between the ground and excited states is very small (see the Supporting Information). Importantly, both **6** and **7** were emissive in the solid state as expected, and the quantum yields (Φ_{FL}) were much higher than those of any solutions of **6** and **7** (AIEE-active[12]) (Figure 4d). Moreover, the λ_{em} of **7** in the solid state (544 nm) was almost the same as that of its cyclohexane solution (527 nm), indicating that **7** rarely interacts electronically with each other in the solid state.

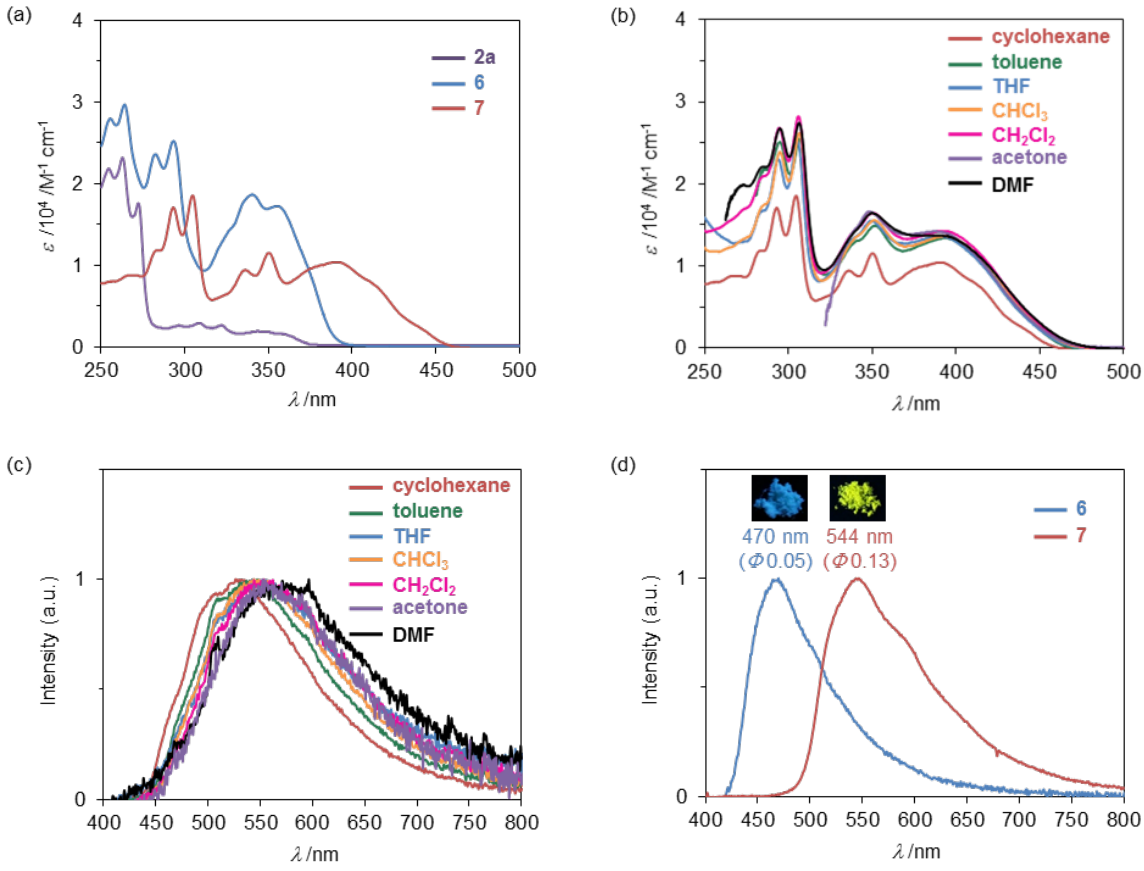

Figure 4. (a) UV-vis absorption spectra of **2a**, **6**, and **7** in cyclohexane (c: 10^{-5} M order); (b) UV-vis absorption spectra of diluted solutions of **7** (c: 10^{-5} M order); (c) Emission spectra of diluted solutions of **7** (c: 10^{-5} M order); (d) Emission spectra of **6** and **7** in the solid state

In conclusion, we have discovered a ring-contractive and -closing skeletal rearrangement of BINAMs induced by an iodine-containing oxidant to give a novel class of spiro aza-heterocycles. Moreover, the utility of a product as a building block for an AIEE-active BF_2 complex has been demonstrated. Further investigation into the creation of functional π-conjugated molecules by making use of the spiro amidino functionality is ongoing in our laboratory.

EXPERIMENTAL

All reactions were carried out under an atmosphere of nitrogen unless otherwise noted. Melting points were determined on a Stanford Research Systems MPA100 OptiMelt Automated Melting Point System. ^{1}H and ^{13}C NMR spectra were recorded on a JEOL JMTC-400/54/SS spectrometer (^{1}H NMR, 400 MHz; ^{13}C NMR, 100 MHz) for **2a**, **2b**, and **2c**, and a Bruker Avance III 600 spectrometer (^{1}H NMR, 600 MHz; ^{13}C NMR, 150 MHz) for **6** and **7**, using tetramethylsilane as an internal standard. ^{19}F NMR spectra were recorded on a Bruker Avance III 600 spectrometer (564 MHz) relative to α,α,α-trifluorotoluene (δ –64.0 ppm in $CDCl_3$). ^{11}B NMR spectra were recorded on a Bruker Avance III 600 spectrometer (192 MHz) using $BF_3{\cdot}Et_2O$ as an external standard. Infrared spectra were acquired on a SHIMADZU IRAffinity-1 FT-IR Spectrometer. Mass spectra were obtained on a JEOL JMS-DX303HF mass spectrometer. High-resolution mass spectra (HRMS) were obtained on a JEOL JMS-DX303HF mass spectrometer. Chiral-phase high-performance liquid chromatography (HPLC) was performed on a SHIMADZU prominence series instruments equipped with chiral columns. Specific optical rotations were measured in a thermostated (20 ˚C) conventional 10 cm cell on a JASCO P-2200 polarimeter using the sodium-D line (589 nm). UV/vis spectra were recorded on a Shimadzu UV-2550 spectrophotometer. Emission spectra were recorded on a HAMAMATSU C11347-01 spectrometer with an integrating sphere. Products were purified by chromatography on silica gel BW-300 and Chromatorex NH (Fuji Silysia Chemical Ltd.). Analytical thin-layer chromatography (TLC) was performed on pre-coated silica gel glass plates (Merck silica gel 60 F_{254} and Fuji Silysia Chromatorex NH, 0.25 mm thickness). Compounds were visualized with UV lamp.

Materials. 1,1'-Binaphthalene-2,2'-diamine (BINAM, **1a)** and (*R*)-BINAM **1a** (99% ee) were purchased from Sigma-Aldrich and used as received. *N*-Iodopyrrolidone (NIPy) was prepared according to the procedures in literature,[26] and other commercial reagents were purchased from Sigma-Aldrich, TCI, or Wako Pure Chemical Industries, Ltd. and used as received. MeCN was purchased as dehydrated grade and dried by passing through a Glass Contour solvent dispensing system (Nikko Hansen & Co., Ltd.). MeOH were dried over activated molecular sieves 3Å. Biaryldiamines **1b**[8] [CAS No. 1656273-33-4], **1c**[27] [CAS No. 861890-12-2], **1d**[28] [CAS No. 1229013-43-7], **1e**[29] [CAS No. 103278-14-4] and **3**[30] [CAS No. 1454-80-4] were prepared according to the procedures in literature. Binaphthalene azide **5** [CAS No.

1620543-69-2] was prepared from 1,1'-binaphthalene-2,2'-diamine (**1a**) according to the procedures in literature.[9]

A Typical Procedure for the Oxidative Rearrangement of Diamines 1. To a two-necked round-bottomed flask (50 mL) equipped with a three-way stopcock and a magnetic stir bar, was added diamine **1a** (56.8 mg, 0.2 mmol) under the air. The vessel was capped with a rubber septum, evacuated, and refilled with N_2 gas for three times, and MeCN (20 mL) was added through the septum. The resulting solution was cooled to –40 °C. To the solution, was added DIH (151.9 mg, 0.4 mmol) under a stream of N_2 gas at –40 °C. The resulting solution was stirred for 7 h before quenched with aqueous $Na_2S_2O_3$ solution (1.0 M, 20 mL), and the resulting mixture was extracted with CH_2Cl_2 (20 mL × 3). The combined organic extracts were dried over Na_2SO_4 and concentrated under vacuum to give the crude product, which was purified by flash column chromatography (eluent: hexane/EtOAc 5:5) on NH silica gel to give product **2a** (38.9 mg, 69%). Further purification was carried out by recrystallization from acetone.

Spiro[benzo[*e*]indole-1,1'-inden]-2-amine (2a). Colorless solid; mp 243 °C (dec.); R_f 0.10 (hexane/EtOAc 5:5 on an NH silica gel plate); ^{1}H NMR (400 MHz, $CDCl_3$) δ 4.80 (br, the peak was too broad to calculate the correct integration), 6.40 (d, J = 5.2 Hz, 1H), 6.71 (d, J = 8.8 Hz, 1H), 6.93 (d, J = 7.6 Hz, 1H), 7.08–7.20 (m, 3H), 7.28 (d, J = 5.6 Hz, 1H), 7.37 (dd, J = 7.6, 7.6 Hz, 1H), 7.56 (d, J = 5.6 Hz, 1H), 7.58 (d, J = 6.4 Hz, 1H), 7.77 (d, J = 8.0 Hz, 1H), 7.82 (d, J = 8.0 Hz, 1H); ^{13}C NMR (100 MHz, $CDCl_3$) δ 70.4, 117.9, 121.2, 122.1, 123.0, 123.1, 125.2, 126.5, 126.8, 128.3, 128.8, 129.0, 129.7, 130.4, 134.9, 138.0, 143.9, 144.5, 155.8, 173.6; IR (ATR) ν 3441, 3305, 3026, 1651, 1622, 1545, 1512, 1452, 1271, 829, 744 cm^{-1}; MS (EI): *m/z* (relative intensity, %) 282 ([M]$^+$, 100), 264 ([$C_{20}H_{10}N$]$^+$, 21), 254 ([$C_{19}H_{12}N$]$^+$, 8), 239 ([$C_{19}H_{11}$]$^+$, 8), 140 ([$C_{10}H_6N$]$^+$, 7); HRMS (EI): *m/z* calcd for $C_{20}H_{14}N_2$ (M) 282.1157, found 282.1160.

*Further experimental information (procedures, compound data, the copies of NMR charts and chiral HPLC charts, crystallographic data, photophysical data) and theoretical results (DFT calculations) are available from the Supporting Information.

ACKNOWLEDGEMENTS

This research was partly supported by the Research Encouragement Grants from The Asahi Glass Foundation (to Y. T.) and Grant-in-Aid for Scientific Research (B) (Grant Number 92073599, to S. M.).

REFERENCES AND NOTES

1. F. Perron and K. F. Albizati, *Chem. Rev.*, 1989, **89**, 1617; R. M. Williams and R. J. Cox, *Acc. Chem. Res.*, 2003, **36**, 127.
2. Y. Zheng, C. M. Tice, and S. B. Singh, *Bioorg. Med. Chem. Lett.*, 2014, **24**, 3673; B. Yu, D.-Q. Yu, and H.-M. Liu, *Eur. J. Med. Chem.*, 2015, **97**, 673.

3. G. B. Bajracharya, M. A. Arai, P. S. Koranne, T. Suzuki, S. Takizawa, and H. Sasai, *Bull. Chem. Soc. Jpn.*, 2009, **82**, 285.
4. T. P. I. Saragi, T. Spehr, A. Siebert, T. Fuhrmann-Lieker, and J. Salbeck, *Chem. Rev.*, 2007, **107**, 1011.
5. M. Sannigrahi, *Tertahedron*, 1999, **55**, 9007; R. Rios, *Chem. Soc. Rev.*, 2012, **41**, 1060; M. A. Borad, M. N. Bhoi, N. P. Prajapati, and H. D. Patel, *Synth. Commun.*, 2014, **44**, 897; M. M. M. Santos, *Tetrahedron*, 2014, **70**, 9735.
6. Y. Takeda, S. Okumura, and S. Minakata, *Angew. Chem. Int. Ed.,* 2012, **51**, 7804; Y. Takeda, S. Okumura, and S. Minakata, *Synthesis,* 2013, **45**, 1029; S. Okumura, C.-H. Lin, Y. Takeda, and S. Minakata, *J. Org. Chem.,* 2013, **78**, 12090.
7. S. Okumura, Y. Takeda, K. Kiyokawa, and S. Minakata, *Chem. Commun.,* 2013, **49**, 9266.
8. Y. Takeda, M. Okazaki, Y. Maruoka, and S. Minakata, *Beilstein J. Org. Chem.*, 2015, **11**, 9.
9. Y. Takeda, M. Okazaki, and S. Minakata, *Chem. Commun.,* 2014, **50**, 10291.
10. D. Sue, T. Kawabata, T. Sasamori, N. Tokitoh, and K. Tsubaki, *Org. Lett.,* 2010, **12**, 256.
11. J.-X. Chen, Y.-Q. Wang, S.-W. Liu, W.-E. Lin, and Z.-P. Chen, *Acta. Cryst.,* 2011, **E67**, o9.
12. Y. Hong, J. W. Y. Lam, and B. Z. Tang, *Chem. Soc. Rev.*, 2011, **40**, 5361; J. Mei, Y. Hong, J. W. Y. Lam, A. Qin, Y. Tang, and B. Z. Tang, *Adv. Mater.*, 2014, **26**, 5429.
13. For a summary of the crystal data of **2a**, see the Supporting Information. CCDC 1416916 contains the supplementary crystallographic data for this paper. These data are available free of charge from the Cambridge Crystallographic Data Center via www.ccdc.cam.ac.uk/data_request/cif.
14. E. D. Raczyńska, M. Makowski, M. Hallmann, and B. Kamińska, *RSC Adv.*, 2015, **5**, 36587.
15. 'CRC Handbook of Chemistry and Physics,' 91st edn., ed. by W. M. Haynes, CRC Press, Boca Raton, FL, 2010.
16. A. Lemmerer and J. P. Michael, *Acta. Cryst.,* 2011, **E67**, o394.
17. The absolute configuration of (–)-**2a** has not been determined, and the absolute configuration shown in Scheme 2b is only conjecture at this moment.
18. N. P. Gritsan and M. S. Platz, *Chem. Rev.*, 2006, **106**, 3844.
19. β-Naphthazirines generated by the decomposition of β-naphthyl azides are known to be nucleophilically attacked by diethylamine to give 1,2-disubstituted naphthalenes: S. E. Hilton, E. V. Scriven, and H. Suschitzky, *J. Chem. Soc., Chem. Commun.,* 1974, 853; M.-L. Tsao and M. S. Platz, *J. Phys. Chem. A,* 2004, **108**, 1169.
20. Y. Sugihara, S. Iimura, and J. Nakayama, *Chem. Commun.,* 2002, 134.
21. E. S. Hand and D. C. Baker, *Synthesis*, 1989, 905.
22. S. Hachiya, T. Inagaki, D. Hashizume, S. Maki, H. Niwa, and T. Hirano, *Tetrahedron Lett.,* 2010, **51**, 1613.

23. Y.-Y. Wu, Y. Chen, G.-Z. Gou, W.-H. Mu, X.-J. Lv, M.-L. Du, and W.-F. Fu, *Org. Lett.,* 2012, **14**, 5226; Y.-Y. Wu, Y. Chen, W.-H. Mu, X.-J. Lv, and W.-F. Fu, *J. Photochem. Photobiol. A,* 2013, **272**, 73; M.-L. Du, C.-Y. Hu, L.-F. Wang, C. Li, Y.-Y. Han, X. Gan, Y. Chen, W.-H. Mu, M. L. Huang, and W.-F. Fu, *Dalton Trans.,* 2014, **43**, 13924.
24. For a summary of the crystal data of **7**, see the Supporting Information. CCDC 1416929 contains the supplementary crystallographic data for this paper. These data are available free of charge from the Cambridge Crystallographic Data Center via www.ccdc.cam.ac.uk/data_request/cif.
25. B. Valeur and M. N. Berberan-Santos, 'Molecular Fluorescence: Principles and Applications,' 2nd edn., WILEY-VCH, Weinheim, 2012.
26. U. Hennecke, C. H. Müller, and R. Fröhlich, *Org. Lett.,* 2011, **13**, 860.
27. P. Yan, A. C. Millard, M. Wei, and L. M. Loew, *J. Am. Chem. Soc.,* 2006, **128**, 11030.
28. C. C. Scarborough, R. I. McDonald, C. Hartmann, G. T. Sazama, A. Bergant, and S. S. Stahl, *J. Org. Chem.,* 2009, **74**, 2613.
29. Š. Vyskočil, M. Smrčina, M. Lorenc, I. Tišlerová, R. D. Brooks, J. J. Kulagowski, V. Langer, L. J. Farrugia, and P. Kočovský, *J. Org. Chem.,* 2001, **66**, 1359.
30. S. Dehghanpour, F. Afshariazar, and J. Assoud, *Polyhedron,* 2012, **35**, 69.